Models of the iron-only hydrogenase: Structural studies of chelating diphosphine complexes $[Fe_2(CO)_4(\mu\text{-pdt})(\kappa^2P,P'\text{-diphosphine})]$†

Fatima I. Adam, Graeme Hogarth,* Idris Richards and Benjamin E. Sanchez

Received 23rd April 2007, Accepted 1st May 2007
First published as an Advance Article on the web 15th May 2007
DOI: 10.1039/b706123b

Six chelating diphosphine complexes, $[Fe_2(CO)_4(\mu\text{-pdt})(\kappa^2P,P'\text{-diphosphine})]$, have been crystallographically characterised allowing differences between basal–apical and dibasal conformations to be analysed.

Dithiolate-bridged diiron complexes, $[Fe_2(CO)_6(\mu\text{-}SCH_2XCH_2S)]$ (X = O, NH, CH_2),[1–20] have been widely studied over the past 7–8 years since they closely resemble the two-iron unit of the H-cluster active site of iron-only hydrogenases.[21–25] Despite significant advances in the understanding of this system a number of limitations still need to be addressed. A major limitation of all current iron-only hydrogenase models is the *unrotated* nature of the two square-planar iron centres. Thus, in current models the two $Fe(CO)_2L$ units roughly eclipse one another (*unrotated*) while in the enzyme they are rotated with one of the carbonyls residing in the area between the two iron centres (*rotated*). A recent theoretical study of the system by Tye, Darensbourg and Hall addressed this issue concluding that "asymmetric substitution of strong donor ligands is the most viable method of making better synthetic di-iron complexes that will serve as both structural and functional models" of the active site of iron-only hydrogenase.[26]

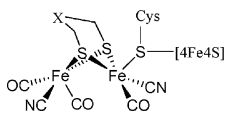

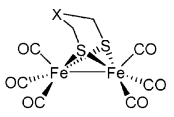

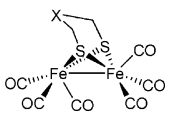

The only structurally characterised model complex to date that fulfils this criteria is $[Fe_2(CO)_3(\mu\text{-pdt})(\mu,\kappa P,\kappa^2P',P''\text{-triphos})]$ (**8**) (H_2pdt = 1,3-propanedithiol, triphos = bis(2-diphenylphosphinoethyl)phenylphosphine) prepared by ourselves from the thermal reaction of triphos with $[Fe_2(CO)_6(\mu\text{-pdt})]$ (**1**).[18] Here the chelating part of the tridentate phosphine adopts a basal–apical coordination geometry in the solid state, while the bridging groups are *cis* basal. In solution, a trigonal twist is believed to interconvert the two basal sites of the dicarbonyl centre, while the trigonal twist of the iron monocarbonyl centre is not observed probably since it leads to an unfavourable twisting of the triphosphine ligand.

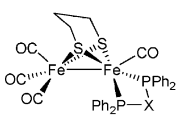

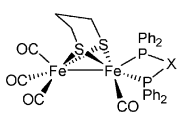

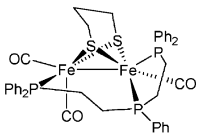

In **8** the relative arrangement of carbonyl ligands at the binuclear centre is strongly dictated by the triphosphine binding mode. This would be less pronounced in tetracarbonyl chelate complexes $[Fe_2(CO)_4(\mu\text{-pdt})(\kappa^2P,P'\text{-diphosphine})]$ since the iron tricabonyl unit would be free to adopt its preferred coordination geometry. In order to probe this, and to assess if significant structural variations result from preferential adoption of a dibasal or apical–basal coordination geometry of the chelating ligand, we have prepared a wide range of complexes of the type $[Fe_2(CO)_4(\mu\text{-pdt})(\text{diphosphine})]$. Herein we report the crystal structures of six tetracarbonyl chelate complexes, $[Fe_2(CO)_4(\mu\text{-pdt})(\kappa^2P,P'\text{-diphosphine})]$, and assess the role the diphosphine coordination plays on the geometry at each metal centre.

Complexes **2–7** were prepared from the reaction of $[Fe_2(CO)_6(\mu\text{-pdt})]$ (**1**) with the relevant phosphine under a range of different conditions‡ and a crystal structure has been carried out on each (Fig. 1 and 2).§ Key metric parametersare given in Table 1 together with data for **1** and **8**. The chelate complexes fall into two structural types. In **2–4**, the diphosphine lies in the basal plane which renders the two phosphorus atoms equivalent, while in **5–7** apical–basal coordination geometry is seen. Dibasal complexes **2–4** are characterised by very small bite-angles of 71.32–74.55° and are adopted by ligands with a single atom linking unit. This leads to quite short phosphorus–phosphorus distances of around 2.6 Å. The thiolate ligands bridge the diiron centre somewhat asymmetrically, bonds to the iron phosphine-substituted centre being around 0.04 Å shorter than those to the iron tricarbonyl unit, which at an average of 2.26 Å are more usual of those found in all basal–apical and other substituted μ-pdt complexes. Basal–apical complexes **5–8** are characterised by significantly larger ligand bite-angles of 86.80–94.96° and the dithiolate ligands bridge approximately symmetrically.

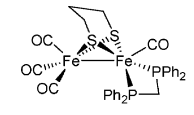

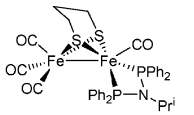

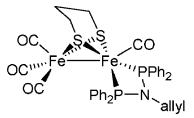

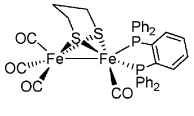

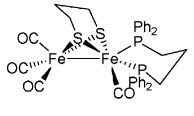

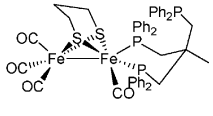

Department of Chemistry, University College London, 20 Gordon Street, London, UK WC1H 0AJ. E-mail: g.hogarth@ucl.ac.uk; Tel: +44 (0)2076794664

† CCDC reference numbers 614428, 614638, 639866–639870. For crystallographic data in CIF or other electronic format see DOI: 10.1039/b706123b

Table 1 Selected metric data [bond lengths (Å) and angles (°)] for diiron μ-pdt complexes

	Fe–Fe	Fe(CO)–S	$Fe(CO)_3$-S	$Fe–P_{basal}$	$Fe–P_{apical}$	Fe–Fe–P	Fe–Fe–C_{apical}	P–Fe–P	τ Fe(CO)	τ $Fe(CO)_3$	Av. torsion angle[c]
1	2.5103(11)		2.2542(10)				148.31(9)			0.070	0
			2.2491(10)								
2	2.5879(7)	2.2222(10)	2.2614(11)	2.2123(11)		107.51(3)	147.87(14)	74.55(4)	0.108	0.314	18.1
		2.2250(10)	2.2650(11)	2.2217(11)		113.56(3)	144.30(15)				
3	2.6236(5)	2.2214(7)	2.2598(7)	2.2124(7)		110.44(2)	138.66(8)	71.32(2)	0.043	0.100	8.5
		2.2203(7)	2.2524(7)	2.2137(7)		107.44(2)	144.71(8)				
4	2.6042(4)	2.2211(5)	2.2637(5)	2.2156(5)		111.38(2)	137.63(6)	71.68(2)	0.008	0.183	11.6
		2.2212(5)	2.2657(5)	2.2172(5)		110.96(2)	145.59(6)				
5	2.5382(6)	2.2616(9)	2.2698(9)	2.2008(9)	2.1843(9)	111.88(3)[a]	148.61(1)	86.80(3)	0.154	0.157	3.3
		2.2587(9)	2.2752(9)			157.34(3)[b]					
6	2.5614(3)	2.2622(4)	2.2623(4)	2.2272(4)	2.2077(5)	110.23(2)[a]	145.45(6)	94.96(2)	0.139	0.160	7.4
		2.2535(4)	2.2623(5)			152.00(2)[b]					
7	2.5778(6)	2.2483(8)	2.2578(9)	2.2241(9)	2.2152(9)	114.39(3)[a]	142.35(11)	90.62(3)	0.287	0.092	6.7
		2.2665(9)	2.2679(9)			151.80(3)[b]					
8	2.5279(5)	2.2589(7)	2.2718(7)	2.1953(7)	2.2016(7)	101.66(2)[a]	154.24(8)	88.37(3)	0.082	0.405	24.5
		2.2644(7)	2.2918(7)	2.2109(7)		109.52(2)[a]					
						156.05(2)[b]					

[a] Basal. [b] Apical. [c] Average torsion angle between *eclipsed* atoms on opposite iron atoms.

Fig. 1 Molecular structure of dibasal **4**.

Fig. 2 Molecular structure of apical–basal **6**.

Introduction of the chelating diphosphine leads to some deviation away from the square-based pyramidal geometry found in **1** and derivatives with monodentate phosphine ligands. Addison, Reedijk and co-workers have developed a simple way of assessing the nature of trigonal bipyramidal and square pyramidal character at a pentacoordinate metal centre.[27] A structural index factor (τ) is expressed as $\tau = (\alpha - \beta)/60$, where α and β are the largest and second largest angles around the metal centre. Thus, $\tau = 0$ is expected for an ideal square pyramidal geometry, while $\tau = 1$ would represent an ideal trigonal bipyramidal structure. The calculated τ values for **1–8** are given in Table 1. The difference between these values for the two iron centres is some measure of the geometric asymmetry induced upon diphosphine chelation. This is a maximum for the triphos complex **8** ($\Delta\tau = 0.323$) and significant differences are also seen in dibasal **2** ($\Delta\tau = 0.206$) and apical–basal **7** ($\Delta\tau = 0.195$) While in all the iron centres are best described as square pyramidal, τ values of 0.314 and 0.287 in **2** and **7** respectively are suggestive of significant trigonal bipyramidal character. Interestingly, while the trigonal bipyramidal character is seen at the iron tricarbonyl unit in dibasal **2**, it is located at the diphosphine-substituted centre in apical–basal **7**. Further, the

greatest asymmetry is seen in **8** where the mono-substituted centre shows significant deviation away from square pyramidal geometry ($\tau = 0.405$).

The chelating phosphines can also be seen to play a role in the eclipsed nature of the three non-sulfur substituents on each metal centre. In **1** the two iron atoms are related by symmetry and thus the three carbonyls on each iron atom are eclipsed.[8] For apical–basal substitution this varies only slightly while for dibasal complexes twisting away from the eclipsed state becomes more pronounced. This is especially so in **2** where the average torsional angle of 18.1° includes angles of 27.7(3) and 20.59° between C(1)–C(2) and P(1)–C(3) respectively. However, the most pronounced distortion away from an eclipsed state is seen in the triphos complex **8** where the torsional angle between P(1)–C(3) is 49.4(2)°, *i.e.* these substituents are virtually staggered (Fig. 3). Despite this asymmetry, however, all these complexes adopt the *unrotated* structure.

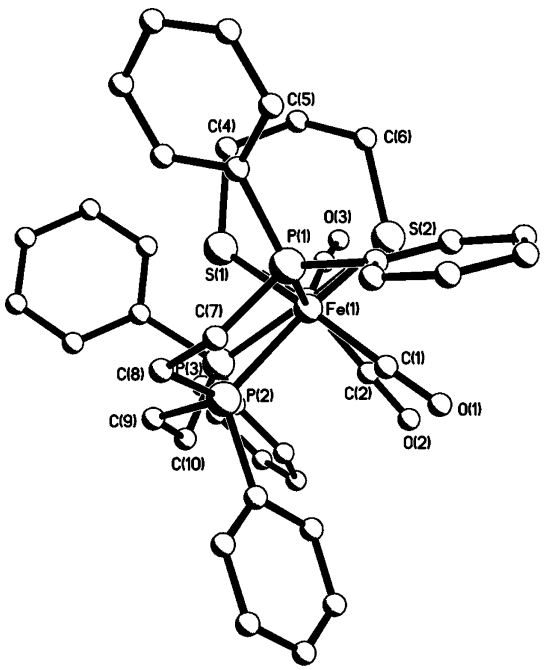

Fig. 3 Molecular structure of **8** looking down the iron–iron vector.

In solution, interconversion of dibasal and apical–basal forms can occur *via* a trigonal twist process. This has recently been shown by De Gioia, Rauchfuss and co-workers to occur in [$Fe_2(CO)_4$(μ-pdt)(κ^2*P*,*P*′-*cis*-$Ph_2PCH{=}CHPPh_2$)][19] which we have independently prepared and characterised.[28] Our structural studies show that this interconversion is associated with a *ca.* 12–25° change in the bite-angle of the diphosphine, which will in turn effect the arrangement of carbonyl ligands.

In conclusion we have reported for the first time the solid-state structures of chelating diphosphine complexes [$Fe_2(CO)_4$(μ-pdt)(κ^2*P*,*P*′-diphosphine)], highlighting how dibasal and apical–basal coordination modes lead to somewhat different structural parameters. This structural asymmetry is matched by an electronic asymmetry across the iron–iron bond, the relatively electron-rich diphosphine-substituted centre being directly coupled to the electron-deficient iron tricarbonyl unit. In the enzyme a similar structural and electronic asymmetry is believed to occur and thus complexes such as those described above may act as more realistic structural and functional models of this important enzymatic site.

Note added in proof.

The X-ray structure of basal–apical [$Fe_2(CO)_4$(μ-pdt)(κ^2-P,P′-$Ph_2PCH_2CH_2PPh_2$)] has been recently reported by Schollhammer and co-workers; S. Ezzaher, J. -F. Capon, F. Gloaguen, F. Y. Petillon, P. Schollhammer, J. Talarmin, R. Pichon and N. Kervarec, *Inorg. Chem.*, 2007, **46**, 3426.

Notes and references

‡ Selected spectroscopic data: **2** IR *ν*(CO) (C_6H_{14}): 2023vs, 1952s, 1917m cm^{-1}; $^{31}P\{^1H\}$ NMR ($CDCl_3$): *δ* 12.5 (s); **3** IR *ν*(CO) (CH_2Cl_2): 2017vs, 1948s, 1895m cm^{-1}; $^{31}P\{^1H\}$ NMR ($CDCl_3$): *δ* 98.2 (s, 80%), 91.6 (s, 20%); **4** IR *ν*(CO) (CH_2Cl_2): 2019vs, 1949s, 1905m cm^{-1}; $^{31}P\{^1H\}$ NMR ($CDCl_3$): *δ* 116.2 (brs, 25%), 100.9 (s, 75%); **5** IR *ν*(CO) (CH_2Cl_2): 2019vs, 1949s, 1906w cm^{-1}; $^{31}P\{^1H\}$ NMR ($CDCl_3$): *δ* 88.1 (s, 90%), 80.5 (s, 10%); **6** IR *ν*(CO) (CH_2Cl_2): 2019vs, 1946s, 1890m cm^{-1}; $^{31}P\{^1H\}$ NMR ($CDCl_3$): *δ* 53.3 (s, 90%), 48.6 (s, 10%); **7** IR *ν*(CO) (CH_2Cl_2): 2020vs, 1949s, 1891m cm^{-1}; $^{31}P\{^1H\}$ NMR ($CDCl_3$): *δ* 56.4 (brs, 75%), 48.4 (brs, 25%), −26.0 (brs); **8** IR *ν*(CO) (CH_2Cl_2): 1947s, 1889vs cm^{-1}; $^{31}P\{^1H\}$ NMR (CD_2Cl_2): *δ* 89.7 (d, *J* 17.2 Hz), 86.3 (dd, *J* 17.2, 9.2 Hz), 83.3 (br), 81.8 (brd, *J* 23.4 Hz), 63.9 (br), 61.6 (d, *J* 9.2 Hz).

§ Crystal data: [$Fe_2(CO)_4$(μ-pdt)(κ^2*P*,*P*′-$Ph_2PCH_2PPh_2$)] (**2**): red block, dimensions 0.14 × 0.13 × 0.11 mm, triclinic, space group $P\bar{1}$, a = 10.3556(13), b = 12.1406(15), c = 12.9298(16) Å, α = 91.174(2), β = 98.599(2), γ = 102.055(2)°, V = 1569.6(3) Å^3, Z = 2, F(000) 732, ρ_{calc} = 1.511 g cm^{-3}, μ = 1.195 mm^{-1}. 12622 reflections were collected, 7042 unique [R(int) = 0.0378] of which 5039 were observed [$I > 2.0\sigma(I)$]. At convergence, R_1 = 0.0543, wR_2 = 0.1253 [$I > 2.0\sigma(I)$] and R_1 = 0. 0826, wR_2 = 0.1387 (all data), for 379 parameters. CCDC 614428. [$Fe_2(CO)_4$(μ-pdt){κ^2*P*,*P*′-$Ph_2PN(Pr^i)PPh_2$}] (**3**): brown block, dimensions 0.24 × 0.16 × 0.14 mm, triclinic, space group $P\bar{1}$, a = 9.7227(10), b = 10.3859(11), c = 18.5263(19) Å, α = 84.913(2), β = 80.645(2), γ = 63.569(2)°, V = 1652.7(3) Å^3, Z = 2, F(000) 780, ρ_{calc} = 1.522 g cm^{-3}, μ = 1.141 mm^{-1}. 14333 reflections were collected, 7563 unique [R(int) = 0.0250] of which 6917 were observed [$I > 2.0\sigma(I)$]. At convergence, R_1 = 0.0421, wR_2 = 0.1095 [$I > 2.0\sigma(I)$] and R_1 = 0. 0453, wR_2 = 0.1122 (all data), for 406 parameters. CCDC 639866. [$Fe_2(CO)_4$(μ-pdt){κ^2*P*,*P*′-$Ph_2PN(CH_2CH{=}CH_2)PPh_2$}] (**4**): red plate, dimensions 0.18 × 0.16 × 0.04 mm, monoclinic, space group $P2_1/n$, a = 9.8036(6), b = 17.9672(12), c = 18.4965(12) Å, β = 100.919(1)°, V = 3199.0(4) Å^3, Z = 4, F(000) 1552, ρ_{calc} = 1.568 g cm^{-3}, μ = 1.178 mm^{-1}. 27778 reflections were collected, 7641 unique [R(int) = 0.0281] of which 6556 were observed [$I > 2.0\sigma(I)$]. At convergence, R_1 = 0.0330, wR_2 = 0.0813 [$I > 2.0\sigma(I)$] and R_1 = 0. 0401, wR_2 = 0.0843 (all data), for 406 parameters. CCDC 639870. [$Fe_2(CO)_4$(μ-pdt)(κ^2*P*,*P*′-$Ph_2PC_6H_4PPh_2$)]·CH_2Cl_2 (**5**·CH_2Cl_2): brown block, dimensions 0.24 × 0.08 × 0.07 mm, monoclinic, space group *Pc*, a = 10.1181(13), b = 10.9537(14), c = 17.301(2) Å, β = 106.262(2)°, V = 1840.7(4) Å^3, Z = 2, F(000) 880, ρ_{calc} = 1.554 g cm^{-3}, μ = 1.174 mm^{-1}. 15525 reflections were collected, 8372 unique [R(int) = 0.0398] of which 7769 were observed [$I > 2.0\sigma(I)$]. At convergence, R_1 = 0.0381, wR_2 = 0.0856 [$I > 2.0\sigma(I)$] and R_1 = 0. 0422, wR_2 = 0.0874 (all data), for 451 parameters. CCDC 639867. [$Fe_2(CO)_4$(μ-pdt){κ^2*P*,*P*′-$Ph_2P(CH_2)_3PPh_2$}] (**6**): red block, dimensions 0.28 × 0.14 × 0.14 mm, triclinic, space group $P\bar{1}$, a = 10.4973(8), b = 11.1050(8), c = 16.5294(12) Å, α = 73.689(1), β = 84.670(1), γ = 61.883(1)°, V = 1628.5(2) Å^3, Z = 2, F(000) 764, ρ_{calc} = 1.514 g cm^{-3}, μ = 1.155 mm^{-1}. 14343 reflections were collected, 7449 unique [R(int) = 0.0160] of which 6774 were observed [$I > 2.0\sigma(I)$]. At convergence, R_1 = 0.0273, wR_2 = 0.0675 [$I > 2.0\sigma(I)$] and R_1 = 0. 0306, wR_2 = 0.0694 (all data), for 525 parameters. CCDC 639868. [$Fe_2(CO)_4$(μ-pdt){κ^2*P*,*P*′-$(Ph_2PCH_2)_3CMe$}] (**7**): red needle, dimensions 0.30 × 0.04 × 0.02 mm, orthorhombic, space group *Pna*2$_1$, a = 23.707(2), b = 16.7698(14), c = 11.2147(10) Å, V = 4458.5(7) Å^3, Z = 4, F(000) 1976, ρ_{calc} = 1.422 g cm^{-3}, μ = 0.896 mm^{-1}. 36380 reflections were collected, 10394 unique [R(int) = 0.0904] of which 7859 were observed [$I > 2.0\sigma(I)$]. At convergence, R_1 = 0.0447, wR_2 = 0.0716 [$I > 2.0\sigma(I)$] and R_1 = 0. 0726, wR_2 = 0.0764 (all data), for 532 parameters. CCDC 639869. [$Fe_2(CO)_3$(μ-pdt){μ,κ*P*,κ^2*P*′,*P*″-$(Ph_2PCH_2CH_2)_2PPh$}] (**8**):[18] orange block, dimensions

0.16 × 0.15 × 0.04 mm, triclinic, space group $P\bar{1}$, $a = 9.4439(8)$, $b = 9.6258(9)$, $c = 22.437(2)$ Å, $\alpha = 99.783(1)$, $\beta = 95.331(2)$, $\gamma = 94.278(2)°$, $V = 1992.8(3)$ Å^3, $Z = 2$, $F(000)$ 948, $\rho_{calc} = 1.536$ g cm^{-3}, $\mu = 1.127$ mm^{-1}. 17384 reflections were collected, 9087 unique [R(int) = 0.0228] of which 7520 were observed [$I > 2.0\sigma(I)$]. At convergence, $R_1 = 0.0405$, $wR_2 = 0.0950$ [$I > 2.0\sigma(I)$] and $R_1 = 0.0510$, $wR_2 = 0.0998$ (all data), for 478 parameters. CCDC 614638.

1 I. P. Georgakaki, L. M. Thomson, E. J. Lyon, M. B. Hall and M. Y. Darensbourg, *Coord. Chem. Rev.*, 2003, **238–239**, 255.
2 D. J. Evans and C. J. Pickett, *Chem. Soc. Rev.*, 2003, **32**, 268.
3 T. B. Rauchfuss, *Inorg. Chem.*, 2004, **43**, 14.
4 L. Sun, B. Åkermark and S. Ott, *Coord. Chem. Rev.*, 2005, **249**, 1653.
5 X. Liu, S. K. Ibrahim, C. Tard and C. J. Pickett, *Coord. Chem. Rev.*, 2005, **249**, 1641.
6 J.-F. Capon, F. Gloaguen, P. Schollhammer and J. Talarmin, *Coord. Chem. Rev.*, 2005, **249**, 1664.
7 J. W. Tye, M. Y. Darensbourg and M. B. Hall, *J. Am. Chem. Soc.*, 2006, **128**, 1552.
8 E. J. Lyon, I. P. Georgakaki, J. H. Reibenspies and M. Y. Darensbourg, *Angew. Chem., Int. Ed.*, 1999, **38**, 3178.
9 E. J. Lyon, I. P. Georgakaki, J. H. Reibenspies and M. Y. Darensbourg, *J. Am. Chem. Soc.*, 2001, **123**, 3268.
10 X. Zhao, I. P. Georgakaki, M. L. Miller, J. C. Yarbrough and M. Y. Darensbourg, *J. Am. Chem. Soc.*, 2001, **123**, 9710.
11 X. Zhao, I. P. Georgakaki, M. L. Miller, R. Mejia-Rodriguez, C.-Y. Chiang and M. Y. Darensbourg, *Inorg. Chem.*, 2002, **41**, 3917.
12 D. Chong, I. P. Georgakaki, R. Mejia-Rodriguez, J. Sanabria-Chinchilla, M. P. Soriaga and M. Y. Darensbourg, *Dalton Trans.*, 2003, 4158.
13 R. Mejia-Rodriguez, D. Chong, J. H. Reibenspies, M. P. Soriaga and M. Y. Darensbourg, *J. Am. Chem. Soc.*, 2004, **126**, 12004.
14 F. Gloaguen, J. D. Lawrence and T. B. Rauchfuss, *J. Am. Chem. Soc.*, 2001, **123**, 9476.
15 F. Gloaguen, J. D. Lawrence, T. B. Rauchfuss, M. Bénard and M.-M. Rohmer, *Inorg. Chem.*, 2002, **41**, 6573.
16 J. Nehring and D. M. Heinekey, *Inorg. Chem.*, 2003, **42**, 4288.
17 L.-C. Song, Z.-Y. Yang, H.-Z. Bian, Y. Liu, H.-T. Wang, X.-F. Liu and Q.-M. Hu, *Organometallics*, 2005, **24**, 6126.
18 G. Hogarth and I. Richards, *Inorg. Chem. Commun.*, 2007, **10**, 66.
19 A. K. Justice, G. Zampella, L. De Gioia, T. B. Rauchfuss, J. I. van der Vlugt and S. R. Wilson, *Inorg. Chem.*, 2007, **46**, 1655.
20 W. Gao, J. Ekström, J. Liu, C. Chen, L. Eriksson, L. Weng, B. Åkermark and L. Sun, *Inorg. Chem.*, 2007, **46**, 1981.
21 Y. Nicolet, C. Piras, P. Legrand, C. E. Hatchikian and J. C. Fontecilla-Camps, *Structure (London)*, 1999, **7**, 13.
22 J. W. Peters, W. N. Lanzilotta, B. Lemon and L. C. Seefeldt, *Science*, 1998, **282**, 1853.
23 B. J. Lemon and J. W. Peters, *Biochemistry*, 1999, **38**, 12969.
24 Y. Nicolet, A. L. De Lacy, X. Vernéde, V. M. Fernandez, E. C. Hatchikian and J. C. Fontecilla-Camps, *J. Am. Chem. Soc.*, 2001, **123**, 1596.
25 H.-J. Fan and M. B. Hall, *J. Am. Chem. Soc.*, 2001, **123**, 3828.
26 J. W. Tye, M. Y. Darensbourg and M. B. Hall, *Inorg. Chem.*, 2006, **45**, 552.
27 A. W. Addison, T. N. Rao, J. Reedijk, J. van Rijn and G. C. Verschoor, *J. Chem. Soc., Dalton Trans.*, 1984, 1349.
28 F. I. Adam, G. Hogarth and I. Richards, unpublished work.
29 S. Ezzaher, J. -F Capon, F. Gloaguen, F. Y. Petillon, P. Schollhammer, J. Talarmin, R. Pichon and N. Kervarec, *Inorg. Chem.*, 2007, **46**, 3423.

